Journal of Machine Engineering, Vol. 11, No. 1-2, 2011

CVD coatings,
fractal and multifractal geometry,
X-ray analyses

Waldemar KWAŚNY[1]

STRUCTURE, PHYSICAL PROPERTIES AND FRACTAL CHARACTER OF SURFACE TOPOGRAPHY OF CVD COATINGS

The aim of the presented study is to establish a methodology elaboration, giving a possibility to predict properties of coatings reached in CVD process on tool materials, based on fractal quantities describing their surface. Coatings' topography and its structure which has an impact on a shape of analysed objects' surface were characterised in a comprehensive way. Influence of a type of process and conditions of deposition over structure and shape of topography as well as mechanical and operational properties of the acquired coatings were determined.

1. INTRODUCTION

Topography of surface of many actual engineering materials, including CVD and PVD coatings, draws a self-similar feature [1-4], what allows to apply the fractal analysis method to their description. As surfaces of actual materials are never perfectly "smooth", so once adequately large enlargement of their fragments is applied, irregularities in the form of valleys and convexities appear. It can be noticed that for some materials, a degree of those irregularities is constant regardless of scale. It means that if analysed surface is smooth and regular, their fragments maintain this feature after being enlarged. When surface is irregular and rough, also its enlarged fragments look the same. It occurs like this, because additional details are disclosed which were not apparent earlier. Fractal geometry is a tool which allows characterizing degree of surface irregularities in qualitative and quantitative way when this value does not depend on scale. The basic fractal quantity that characterizes efficiency of space filling by surface and describes its shape is the surface fractal dimension - D_s. The fractal dimension D_s, being a real number in interval [2],[3] is a measure of irregularities and a degree of complexity of surface shape. Low value of fractal measure is characteristic for smooth surfaces, whereas high value describes surfaces of complex and complicated shape. Practically, as early as the theory of fractals was established, B.B.

[1] Institute of Engineering Materials and Biomaterials, Silesian University of Technology, ul. Konarskiego 18a, 44-100 Gliwice

Mandelbrot [5] indicated that, for description of the majority of actual objects (he chose distribution of copper deposits for example), application of the fractal formalism is insufficient. It results from a fact that actual objects are not homogenous, and because of that, it is impossible to describe geometrical features of objects of irregular shapes (except for the abstract mathematical constructions) with the help of one number – the fractal dimension. Surfaces of investigated engineering materials usually are not ideal self-similar objects, because that feature occurs only locally. Irregularities distribution changes depending on analysed fragment selection of a sample area. In some fragments, surfaces can be characterized by high irregularity, whereas they may reveal a more regular shape in the others. Mandelbrot has proposed to generalize a concept of the fractal set and replace it by a multi-fractal measure. The multi-fractal measure enables to characterize complex shapes, including surface, for which determined dimension adopts different values in different areas. Therefore, a multi-fractal analysis is an extension of the fractal method, enabling to characterize the geometrical features of actual surfaces in more complete and accurate way [6[,[7].

2. MATERIAL FOR STUDIES

Studies are performed on:

- Multi-edge inserts made of silicon nitride ceramics Si_3N_4.
- Multi-edge inserts made of oxide tool cermets Al_2O_3+ZrO_2.
- Multi-edge inserts made of oxide tool cermets Al_2O_3+TiC.
- Multi-edge inserts made of oxide tool cermets Al_2O_3+SiC.

uncovered and covered in CVD process with single and multi-layer coatings resistant to abrasion (Tab. 1).

Table 1. Characteristics of the investigated coatings obtained in CVD process

No.	**Material of substrate**	**Type of coating**
1	Si_3N_4	TiN+Al_2O_3
2	Si_3N_4	TiN+Al_2O_3+TiN
3	Si_3N_4	TiN+Al_2O_3+TiN+Al_2O_3+TiN
4	Si_3N_4	Al_2O_3+TiN
5	Si_3N_4	TiC+TiN
6	Si_3N_4	Ti(C,N)+TiN
7	Si_3N_4	Ti(C,N)+Al_2O_3+TiN
8	Si_3N_4	Ti(C,N)+Al_2O_3
9	Al_2O_3+ZrO_2	TiN+Al_2O_3
10	Al_2O_3+ TiC	TiN+Al_2O_3
11	Al_2O_3+ $SiC_{(w)}$	TiN+Al_2O_3

3. STUDY METHODOLOGY

Structure of generated coatings was observed at lateral fractures were observed with a Carl Zeiss ULTRA 35 Field-Emission Scanning Electron Microscope (SEM) equipped with energy-dispersive X-ray spectroscopy (EDS). For imaging SEM, a lateral (SE) and In-lens detector using secondary electrons detection at accelerating voltage in a range of 1-20 kV were applied.

Investigations for material surface topography of substrates and generated coatings are carried out in an exchanged scanning electron microscope and using a method of atomic force microscopy (AFM) on a unit of Nanoscope E made by Digital Instruments company. For each of analyzed surface, six measurements are made at scanning range of 5 μm.

X-rays studies for the analyzed materials are carried out on X´Pert PRO system made by Panalytical Company using filter radiation of a cobalt anode lamp. A phase analysis of the analysed materials is carried out in Bragg-Brentano geometry (XRD) using a Xcelerator strip detector, and in grazing incidence geometry (GIXRD) of primary beam using a collimator of parallel beam before a proportional detector.

Measurements of stresses for the analyzed coatings were made by $\sin^2\psi$ and/or g-$\sin^2\psi$ technique depending on the investigated samples properties on the basis of X'Pert Stress Plus company's. In the method of $\sin^2\psi$, based on diffraction lines displacement effect for different ψ angles, appearing in the conditions of stress of materials with crystalline structure, a silicon strip detector was used at the side of diffracted beam. Samples inclination angle ψ towards the primary beam was changed in the range of 0° ÷ 75°. Moreover, measurements of stresses are made by a diffraction technique in grazing incidence geometry using a collimator of a parallel beam in front of the proportional detector [8, 9].

Selection of incident angle of the primary beam (α_x = 0,5°; 1°; 2°; 3°; 5°; 7°) was mainly dependant on linear absorptivity and combination of the applied layers, but the effective X-rays penetration depth g is estimated on the basis of the following dependence:

$$g = \left(\frac{\mu}{\sin\mu} + \frac{\mu}{\sin(2\theta_{\{hkl\}} - \alpha_x)}\right)^{-1} \tag{1}$$

where:
μ – linear absorption of the X-rays,
α_x – incident angle of the primary beam.

Microhardness investigations for investigated coatings and substrates hardness are conducted by means of an ultramicrohardness tester - DUH 202 manufactured by Shimadzu using Vickers method at load of 0.07 N.

Assessments for coatings adhesion to the substrate's material were made by a drawing method on Revetest device manufactured by CSEM.

Roughness investigations for the generated coatings and substrates surface were carried out on Stronic3 profile measurement gauge + Taylor-Hobson companies. R_a quantity is adopted as a value, which determined the surface roughness in accordance with PN-EN ISO 4287. Plates life

without coatings and with deposited coatings in a high-temperature CVD process are determined on the basis of technological cutting test in room temperature. Cutting ability test for investigated materials is made as a continuous turning method at PDF D180 loathe without cutting fluids. The material subjected to machining was grey cast iron EN-GJL-250 of hardness approx. 215 HBW.

Life of plates is determined based on wear bandwidth measurements upon flank face, measuring a mean bandwidth wear VB after machine cutting in specified period of time. Cutting tests were stopped, when VB value exceeded an assumed criterion (VB = 0.3 mm), both for uncovered tools and deposited coatings tools. VB measurements with an accuracy of up to 0, 01 mm were made employing a Carl Zeiss Jena light microscope.

Indication of the fractal dimension and the multi-fractal analysis for investigated materials is carried out on the basis of optical measurements in atomic force microscope AFM, being grounded on projective covering method [10]. In the course of this analysis, N_s=512x512 measurements of a sample height h_i are made, where the first number determines an amount of lines to be scanned, whereas the second one is a number of measuring points in each of them. A distance between the lines and the measuring points is constant and the same.

The measurements, which are carried out, using an atomic force microscope AFM enabled furthermore, indication of a quantity determined as R_{2D} and characterizing roughness for analysed sample surface. R_{2D} roughness is determined in two stages. In the first one, each set of measurements results for the h_i sample height is approximated by the regression plane of H(x, y), for which a sum of squares of the distance from experimental data is minimal, and then, a roughness quantity value R_{2D} is determined for the analyzed sample surface on the ground of a dependency:

$$R_{2D} = \left[\frac{\sum_i (h_i - H_i)^2}{N_s} \right]^{\frac{1}{2}} \tag{2}$$

where:

N_s – number of measuring points,
h_i – sample height at *i* point,
H_i – value of H(x, y) at *i* point.

Application of the above procedure eliminated influence of sample inclination (levelling error) over an acquired value of calculated quantity.

To verify significance of the product-moment correlation coefficients of the obtained results in mechanical, applicable and fractal studies, t statistics is used being subject to Student's distribution with a number of independent variables equals n – 2, where n is a number of measurements. Analyses were performed at the level of significance α_{stat}=0.05. Empirical value for the test statistics t was determined in accordance with a formula:

$$t = \frac{r}{\sqrt{1 - r^2}} \sqrt{n - 2} \tag{3}$$

where, r is an empirical Pearson product-moment correlation coefficient, based on a random sample. The symbol $t_{critical}$ standing for a critical value, read out of tables for the test statistics distribution. Decision about a possible null hypothesis rejection (lack of correlations), was taken on the ground of the result for empirical value comparison of the test statistics with a critical value, read out from distribution tables of the test statistics. If $|t| > t_{critical}$, the null hypothesis on lack of correlations was rejected as statistically less probable and the alternative hypothesis on correlations significance was accepted [11].

4. INVESTIGATIONS RESULTS AND DISCUSSION

The performed metallographic studies allow to state that the tested oxide ceramic tool materials on the basis of Al_2O_3, nitride tool ceramics Si_3N_4, and tool cermets are characterized by compact structure. As a result of factographic investigations performed on a scanning electron microscope for the analysed CVD coatings, it was found that the deposited coatings determine single, double, or multilayer structure depending on applied system of layers, and particular layers are uniformly deposited and tightly adhere to each other as well as to the substrate's material. Observations of surface topography for the analysed coatings using scanning microscopy demonstrate that the observed characteristic columns endings located on surface, forming appropriate coatings, have a shape of reversed pyramids, cones, polyhedrons or craters. However, it is difficult unequivocally to indicate differences among particular coatings in terms of quality and quantity on the basis of observations of the received topography images for the analysed surfaces (Fig. 1). The EDS chemical composition studies of coatings obtained in high-temperature CVD processes confirm proper elements appearance in any analyzed layers, whereas for the sake of low thickness of the deposited layers and characteristics of incident beam, in some cases the applied method allows for a mean measurement of scattered X-rays radiation energy for two or more layers of the investigated coating.

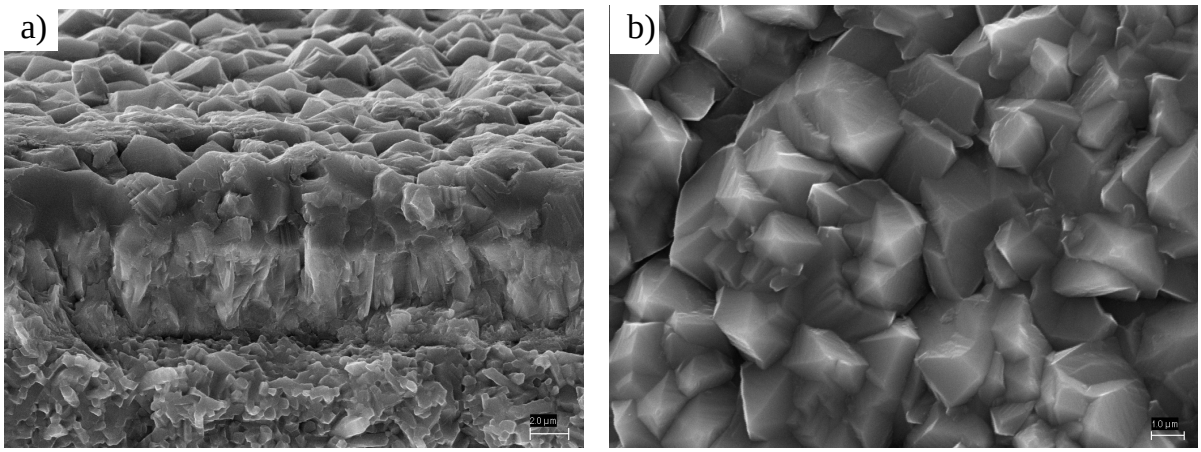

Fig. 1. a) Brittle fracture of a coating $TiN+Al_2O_3$ received on a substrate made of tool ceramics Al_2O_3+SiC in high-temperature CVD process and b) its picture corresponding to surface topography

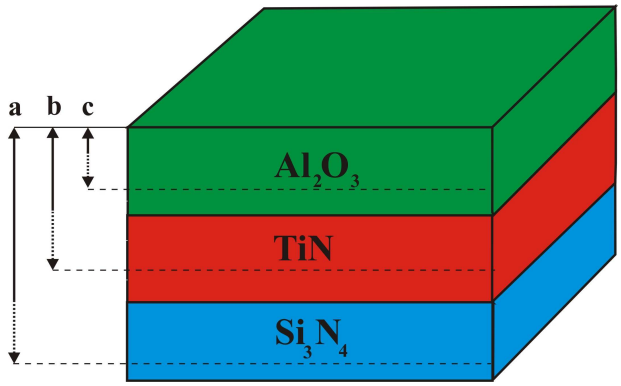

Fig. 2. Scheme for layers on-lapping/packing on a TiN+Al_2O_3 coating received in high-temperature CVD process made of nitride ceramics Si_3N_4 and areas covered by diffraction depending on applied geometry measurement: a) Bragg-Brentano geometry, b) in grazing incidence geometry, α_x = 3°, c) in grazing incidence geometry, α_x=1°

The applied method of X-ray qualitative phase analysis carried out in Bragg-Brentano geometry confirms occurrence of appropriate phases in the investigated substrates and coating materials. Some of identified reflexes on analysed diffraction patterns are moved towards lower or higher angles of reflection as well as their intensity differ from values given in JCPDS card files, what may indicate on occurrence of texture as well as of compressive or tensile, internal stresses in the investigated coatings – a fact one can come across frequently in coatings deposited by the PVD and CVD [12],[13] technique. For the sake of reflexes overlapping of material substrate and coating/coatings, as well as their intensity, making sometimes the analysis of obtained results more difficult; and in order to acquire more accurate information from subsequent layers of the analyzed materials, additional technique of diffraction is applied at grazing incidence geometry (GIXRD), for the primary X-rays beam using a parallel beam collimator in front of proportional detector. Thanks to the possibility to register the diffraction patterns at low incidence angles of the primary beam onto the test piece surface, one can obtain the diffraction lines from thin layers due to volume growth of the material participating in diffraction and acquiring information on the changing phase composition at different depths of the examined material – which do not exceed the rays beam penetration depth when their incident angle is perpendicular to the test piece [14]. Carried out investigations at such assumptions confirm the right sequence of layers (Fig. 2-4) in analyzed coatings.

So that deposited coating on a tool could properly fulfil its task, it has to be characterized by suitable usable properties determined by numerous factors, among which the following should be specified: appropriate structure, chemical and phase composition, proper hardness and thickness, and above all, high adhesion to substrate's material. Adhesion dependence of the analysed coatings for substrates material on conditions of a process needed to obtain them is evaluated by a "scratch test" method at changing load, establishing a value of critical load L_c, allowing to determine a force value inducing the coating damage (Table 3). The critical value L_c is settled as adequate to growth of acoustic emission intensity, signalling fraction imitation of coating.

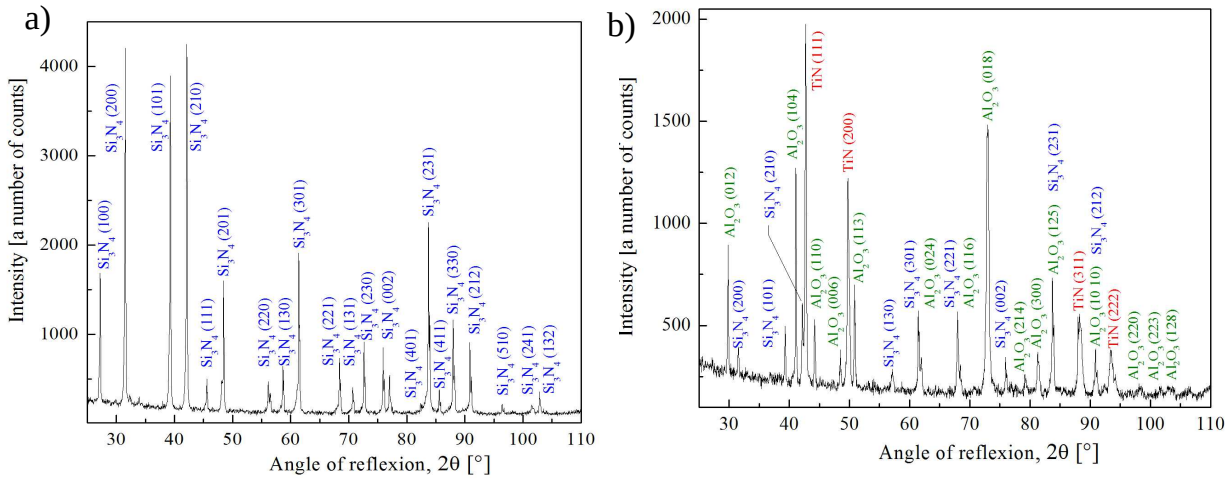

Fig. 3. X-rays diffraction patterns acquired in Bragg-Brentano geometry a) nitride ceramics and b) TiN+Al_2O_3 coatings obtained in high-temperature CVD process on a substrate made of Si_3N_4

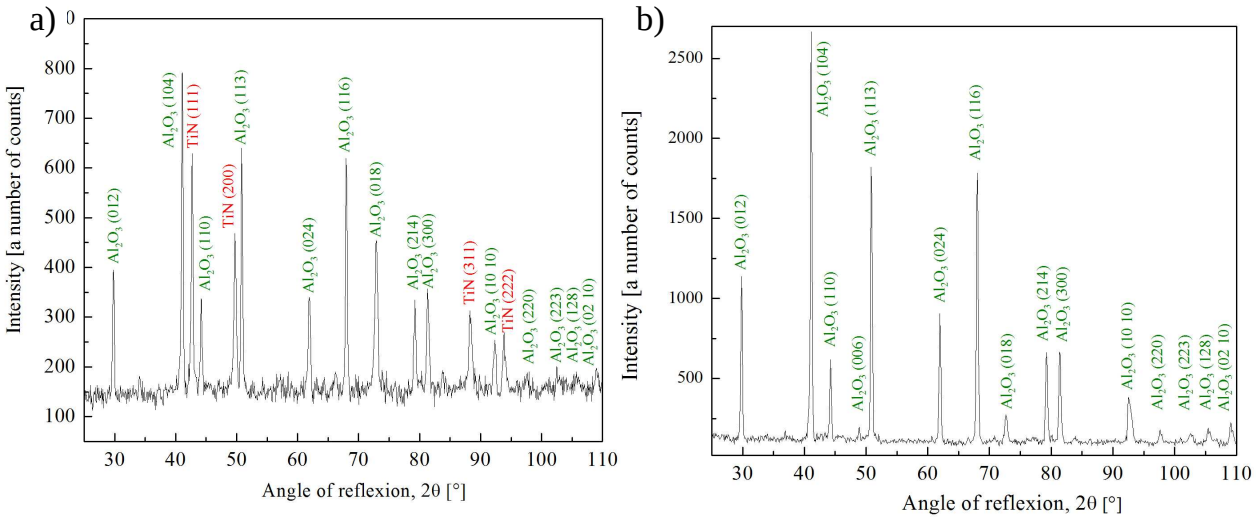

Fig. 4. X-rays diffraction patterns of TiN+Al_2O_3 coating obtained in high-temperature CVD process on a substrate made of nitride ceramics Si_3N_4 received in geometry of constant angle of incidence: a) GIXRD method, α_x = 3º, b) GIXRD method, α_x = 1º

Stresses' measurements of the analyzed materials are performed by two methods, and obtained results are presented in Tables 4 & 5. Stresses' measurements by $\sin^2\psi$ method are made for three φ angles of samples arrangement towards an initial configuration, in which goniometer axis was in two opposite directions continuously (φ = 90 & 270°, φ = 150 & 330°, φ = 210 & 30°). Applying this geometry of measurement enables to observe changes of state of stress for chosen directions of investigated material and to determine its highest value [15-17]. For coatings acquired in the high-temperature CVD process, stresses are defined on the ground of analysis of reflex displacement recorded at the highest value of 2Θ angle, free from influencing on its shape and location of the other components of the investigated material (substrate's material, possible other layers included

in the coating). Locations of the recorded reflexes were determined by a Gaussian curves matching method. In the method of $\sin^2\psi$, to assess stresses, the reflexes recorded at higher values of the angle 2θ are preferred considering higher deformations sensitivity and lower error of obtained results, however, it is not always possible to achieve that in experimental studies, when too low peaks intensity, resulting from texture of analyzed coatings, extensive or irregular shape and relatively small depth of penetration of X-rays radiation at high angles of reflexion make impossible correct and proper assessment. In case of studying multi-layer coatings and/or coatings of phase composition close to the substrate's material, applying this geometry of measurement not always guarantees reception of correct results of measurements as a result of particular components reflexes overlapping of the investigated materials. Because of this, measurements of the analyzed coatings stresses are conducted additionally by a method of g-$\sin^2\psi$. The method g-$\sin^2\psi$ defining stresses based on geometry of a constant incidence angle was proposed by Van Hacker [18], Quaeyhaegens and Knuyt [19], and then, it was expanded by Skrzypek. Finally, algorithm for calculations of stresses was applied by Skrzypek and Baczmański [20],[21]. The method of g-$\sin^2\psi$ is characterized by the use of many diffraction lines from planes {hkl} in contradiction to a classical method of $\sin^2\psi$, using one diffraction line [22]. The main advantage of the method g-$\sin^2\psi$ in reference to the classical method $\sin^2\psi$ measuring stresses, where we are engaged in variable, effective depth of penetration of X-rays radiation into the investigated material, it is almost a constant value for a fixed value α_x , which can be changed by incidence angle or selection of different type of radiation. Moreover, in this method, changing reflexes {hkl} for a crystallographic plane are simultaneously used in a measuring procedure to determine stresses and the method can be easily applied for changing geometries of measurement [21],[22]. Each time measurements of stresses were carried out upon external coating, and as far as it was possible, depending on a type of substrate's material, properties and configurations of the applied layers, in a coating adhering to it, using one or two non-destructive methods to measure this size. The carried out investigations results for internal macro-stresses (defined by the g-$\sin^2\psi$ method) in TiN+Al_2O_3 coatings acquired in the CVD process show dependencies between coatings' stresses size and their adhesion to substrate's material (Fig. 5a). An adhesion value to the substrate's material from stresses appearing in coatings can be defined by the following analytical dependence: y= -0.1443x-0.8489 (Fig. 5b). Assessing a dependence between stresses occurring in external layer made of Al_2O_3 and its adhesion to the substrate's material, the following high correlation was found (correlation coefficient r=0.960) and essential one (t=4.871 towards $t_{critical}$=4.303).

Depending on their value, internal stresses can affect the substrate – coating arrangement unfavourably or positively, and by extension, they can decide about application of produced tools afterwards. Compressive stresses (Fig. 6a & 7a – "negative" slope of a line acquired while stresses measuring) increase crack resistance and to some degree, dependent on thickness, phase and chemical composition as well as material, at which they have been reached, minimize a coating chipping increasing their adhesion to substrate. The opposite type of stresses (Fig. 6b & 7b – "positive" slope of a line acquired while stresses measuring), compressive stresses can accelerate destruction of a coating while imposing

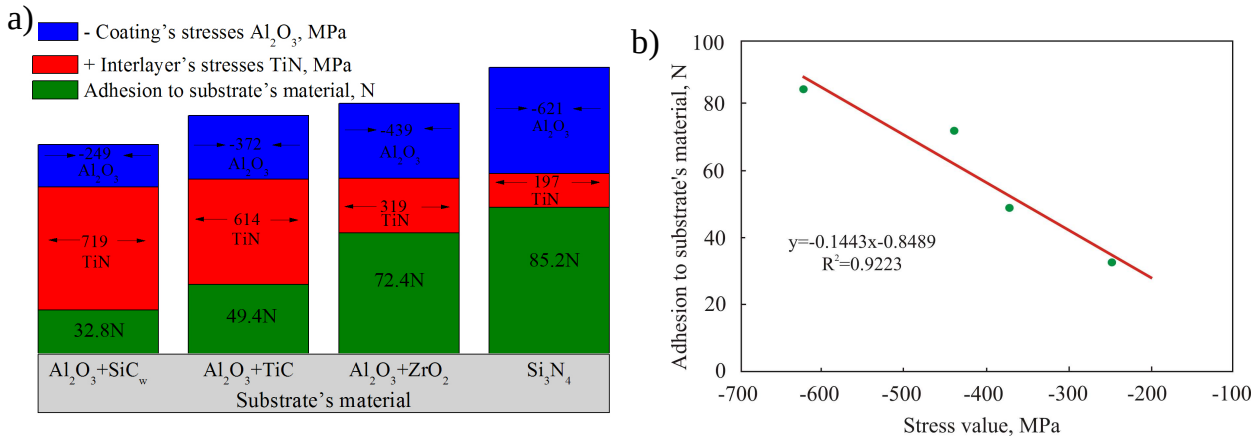

Fig. 5 a) A scheme for stresses influence defined by the method of g-sin$^2\psi$ in the intermediate inter-layer and external coating on adhesion of TiN+Al_2O_3 coatings depending on substrate's material b) Adhesion dependence on stresses' values defined by the method of g-sin$^2\psi$ in the external coating of TiN+Al_2O_3 coatings

an external load. A very important factor having an impact on state of internal stresses in coatings is their structure, which is strictly related to a technique obtaining them, by phase and chemical composition, texture, process temperature and type of substrate, on which it was obtained. Besides, increase of stresses' value along with coatings' thickness was found, analyzing and comparing layers of close phase composition obtained on the same substrate; this phenomenon was described by Thornton and Hoffman in their thesis [23]. While adhesion scratch test is carried out, shearing stress in a transition zone is induced by influence of a loaded penetrator in a normal direction on a coating – substrate configuration. The stresses caused by pressure/thrust of a shifting penetrator are transferred by a coating to the transition zone. Thicker coatings, in this case, require higher load to get the same shearing stresses in the transition zone between the coating and the substrate's material. Comparing both techniques of measurement of stresses (Table 2), it was found that its proper selection depends, in a large

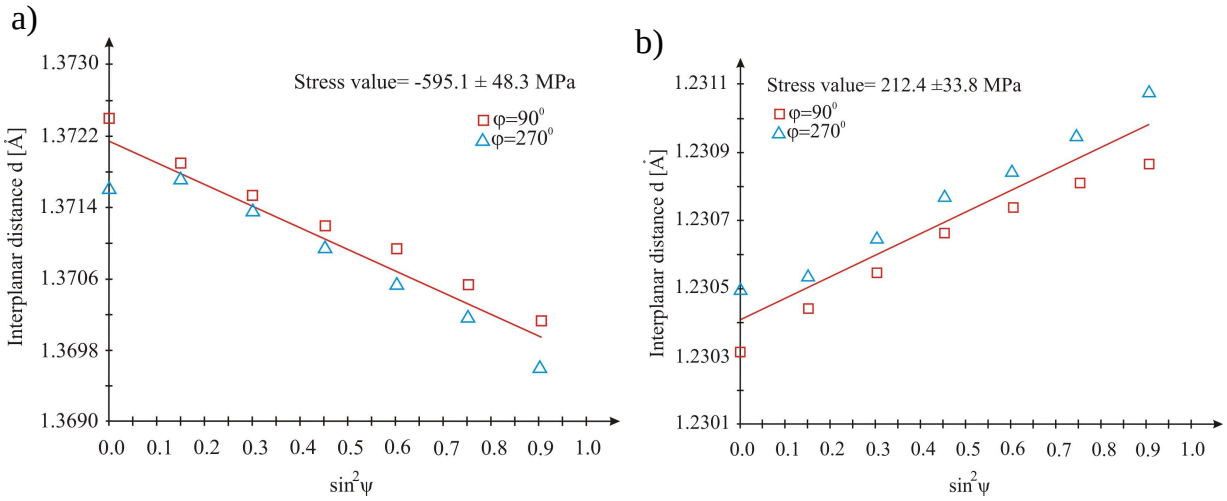

Fig. 6. Changes of interplanar distance value d a) of reflex (300) in the layer Al_2O_3 as and b) reflex (300) of intermediate TiN layer a function of sin$^2\psi$ (stresses' measurement made by sin$^2\psi$ method for different φ values of samples setting towards goniometer axis, TiN+Al_2O_3 coating obtained on a substrate made of nitride ceramics - Si_3N_4)

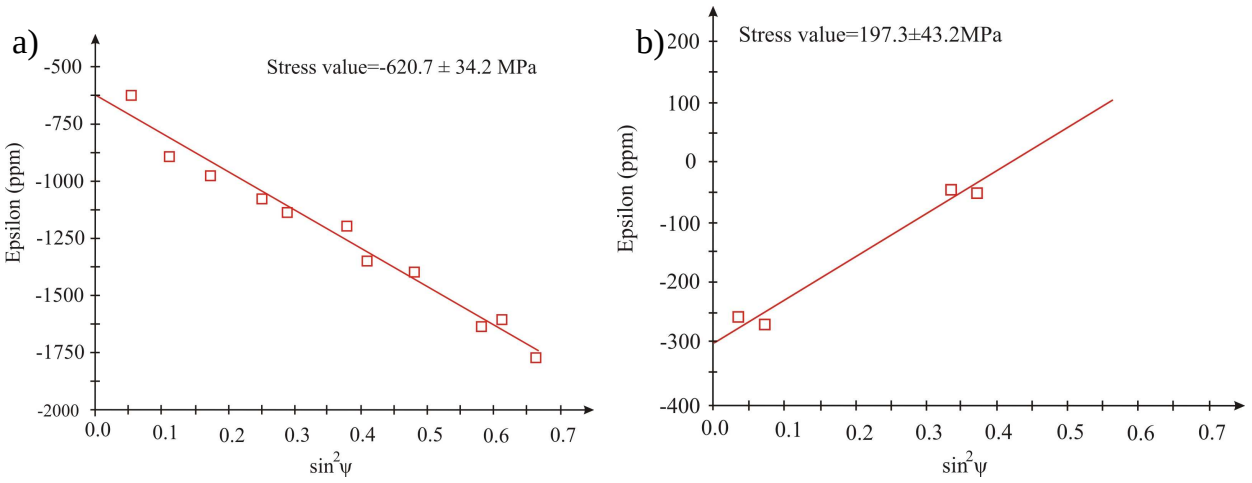

Fig. 7. Changes of the epsilon values (ppm) specifying crystallographic lattice deformation for a) Al_2O_3 layer and b) TiN layer in a function of $\sin^2\psi$ (stresses' measurement by the method of g-$\sin^2\psi$, coating TiN+ Al_2O_3 obtained on a substrate made of nitride ceramics Si_3N_4)

degree, on structure and properties of investigated materials. For coatings, not determined by texture, consisting of many layers giving many diffraction reflexions, it is strongly recommended to apply the method of g-$\sin^2\psi$, where measurement results of stresses are burden with a less-important mistake, whereas in some cases they are impossible to get by a classical method. The perfect example is the obtained results of stresses' measurement of coatings acquired in the high-temperature CVD process, where the analyzed coating was Al_2O_3, for the sake of lack of texture and relatively great number of diffraction reflexes from one phase in reference to the others.

The received analyses are shown in the form of graphs depending on wear bandwidth at VB flank face in a function of test duration at specified conditions to execute the experiment, and the obtained results are of comparative character. Based on technological turning test, the most distinctive improvement tool life, comparing TiN+Al_2O_3 coatings obtained on different substrates as well as coatings obtained on substrates made of nitride ceramics Si_3N_4 (Fig. 8) acquired in the high-temperature CVD process respectively, when the substrate's material was tool ceramics Si_3N_4 and external Ti(C,N)+Al_2O_3 coating. Above-mentioned coatings are characterized by very good adhesion to substrate's material and high microhardness. High adhesion of the analyzed coatings, defined by load value L_c responsible for coating's destruction is adequately 85,2 & 68,3 N, and compressive stresses value is defined by g-$\sin^2\psi$ method, adequately -595 & -421 MPa. In the Table 3, measurements results of mechanical and operational properties are presented for coatings acquired in the CVD process. As a result of a metallographic analysis, conducted on a scanning electron microscope, it was found that the most frequently occurring types of tribological damages, identified on investigated materials are mechanical and frictional damages, as well as thermal cracks of the surface flank, crater forming on surface of attack and a chip build-up on a cutting edge (Fig. 9) [24-26].

Table 2. Results for stresses' measurement of coatings obtained the high-temperature CVD process made by method $\sin^2\psi$ & g-$\sin^2\psi$

Substrate's material	Type of coating (layers configuration)	Coating thickness [μm]	Type of coating, from which information came (external/ indirect)	Method $\sin^2\psi$, [MPa]	Method g-$\sin^2\psi$, [MPa]
Si_3N_4	TiN+Al_2O_3	9,6	Al_2O_3	-595±48	-621±34
			TiN	212±34	197±43
Si_3N_4	TiN+Al_2O_3+TiN	3,8	TiN	-	-97±43
			Al_2O_3	-99±34	-151±23
Si_3N_4	TiN+Al_2O_3+TiN+ Al_2O_3+TiN	5,1	TiN	-	-120±32
			Al_2O_3	-	-191±26
Si_3N_4	Al_2O_3+TiN	2,7	TiN	69±61	-89±59
			Al_2O_3	-105±32	-123±21
Si_3N_4	TiC+TiN	5,4	TiN	-59±29	-49±43
			TiC	-142±33	-129±41
Si_3N_4	Ti(C,N)+TiN	4,2	TiN	-	-89±42
			Ti(C,N)	-	-219±52
Si_3N_4	Ti(C,N)+Al_2O_3+TiN	9,5	TiN	-	-69±34
			Al_2O_3	-	-108±27
Si_3N_4	Ti(C,N)+Al_2O_3	5,2	Al_2O_3	-452±43	-421±29
			Ti(C,N)	-86±55	-76±33
Al_2O_3+ZrO_2	TiN+Al_2O_3	6,4	Al_2O_3	-	-439±27
			TiN	-	319±56
Al_2O_3+TiC	TiN+Al_2O_3	5,3	Al_2O_3	-	-372±33
			TiN	-	614±52
Al_2O_3+$SiC_{(w)}$	TiN+Al_2O_3	7,3	Al_2O_3	-	-249±29
			TiN	-	719±58

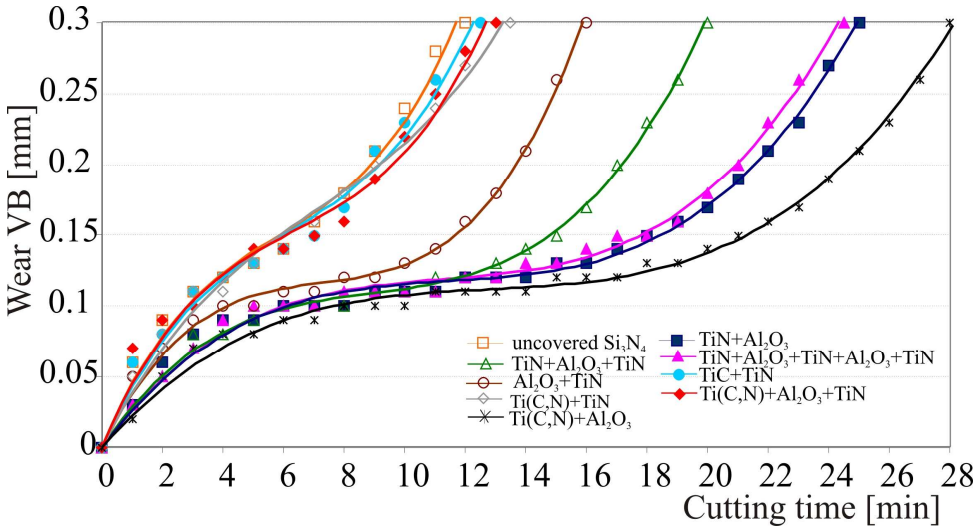

Fig. 8. Graphs of wear bandwidth dependencies on a VB flank face of cutting time for coatings obtained in the high-temperature CVD process on a substrate made of ceramics Si_3N_4

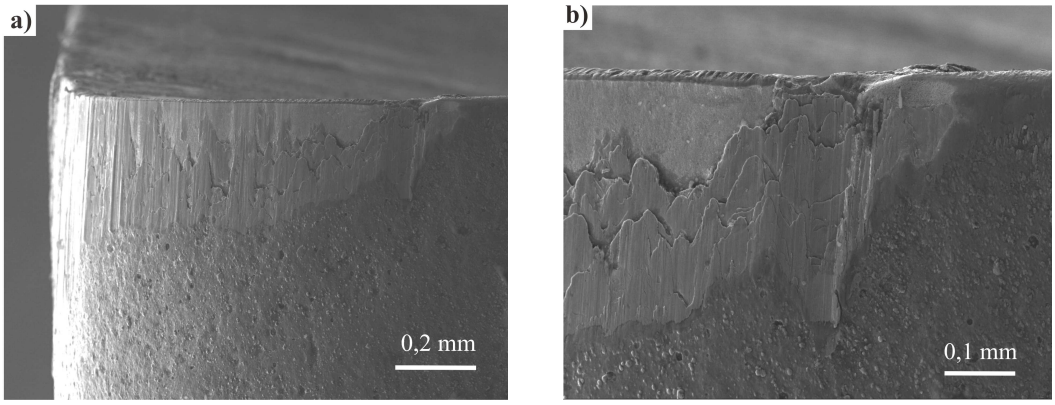

Fig. 9. a) A view of tool ceramics flank face wear made of Al_2O_3+SiC with a deposited coating TiN+Al_2O_3 b) detail from a drawing a

Table 3. Results of mechanical and operational measurements for substrates' material as well as coating obtained in the high-temperature CVD process

Substrate's material	Type of coating	Roughness R_a [μm]	Microhardness $HV_{0,07}$	Adhesion N	Operational properties	
					Tool life T (min)	Increase (%)
Si_3N_4	TiN+Al_2O_3	0,45	3250	85,2	25	108
Si_3N_4	TiN+Al_2O_3+TiN	0,13	2800	50,4	20	67
Si_3N_4	TiN+Al_2O_3+TiN+Al_2O_3+TiN	0,52	3050	55,7	24,5	104
Si_3N_4	Al_2O_3+TiN	0,23	2700	29,1	16	33
Si_3N_4	TiC+TiN	0,25	2050	25,8	12,5	4
Si_3N_4	Ti(C,N)+TiN	0,15	2225	34,1	13,5	13
Si_3N_4	Ti(C,N)+Al_2O_3+TiN	0,28	2030	30,8	13	8
Si_3N_4	Ti(C,N)+Al_2O_3	0,25	3250	68,3	28	133
Al_2O_3+ZrO_2	TiN+Al_2O_3	0,43	3400	72,4	20,5	86
Al_2O_3+TiC	TiN+Al_2O_3	0,29	3350	49,4	24,5	81
Al_2O_3+$SiC_{(w)}$	TiN+Al_2O_3	0,44	3100	32,8	24	33
Si_3N_4	-	0.08	1870	-	12	-
Al_2O_3+ZrO_2	-	0.21	1850	-	11	-
Al_2O_3+TiC	-	0.09	1970	-	13.5	-
Al_2O_3+$SiC_{(w)}$	-	0.26	1870	-	18	-

In the herewith evaluation to determine the fractal dimension of coatings surfaces, a modified method for projective covering (PCM) was applied [10]. The PCM method was evaluated at the end of the last century and used for determining the fractal dimension of surface of rocks, and then, it was used many a time in studies for surface of diverse engineering materials [27-32].

Three dimensional images of coatings surface topography obtained based on data from measurements made by means of on AFM microscopes are precious source

of information on shape of surface, however, their interpretation and comparison are difficult, subjective and often lead to false conclusions. Appearance of those graphs, in a large degree, depends on the way they are presented (applied colours and their intensity, perspective, and the like) and applied scale in z axis. Simultaneously, applying a rule that for all compared samples in z axis the same unit appears, especially a unit equal to a unit occurring in x and y axes, make the graphs more illegible. For the sake of images of coatings surface topography received based on data coming from measurements made on AFM microscopes, they can only give an idea about shape of surface, but they should not used in highly advanced analyses.

Making measurements on the AFM microscope and getting digital recording of topography of the analyzed surfaces created a possibility to determine two-dimensional quantity of roughness R_{2D}, which in comparison with classical quantities determined along one segment, enables to obtain more representative values. The roughness quantity is a commonly used value defining shape of surface, and first of all, it should be considered when comparing and assessing the shape of coatings. R_{2D} roughness determined based on measurements made by the AFM microscope is an informing quantity on, in what degree the analyzed area differs from the flat surface, but it does not indicate what made this difference, whose source might be of two different factors:

- Surface waviness (irregularity occurrence of high amplitude),
- Appropriate roughness (densely arranged irregularity occurrence of low amplitude).

The fractal analysis enables to differentiate those factors, and additionally, thanks to determining the multi-fractal spectrum, to assess homogeneity of the analysed objects.

Points arrangement on the bilogarithmic plot is defined by a degree of an analysed surface development, and simultaneously it indicates factors which have influence on it: surface waviness or appropriate roughness. On the ground of the bilogarithmic plot also fractality of the analysed set of data is assessed. Performing an auxiliary plot facilitates the right selection of the fractality range or taking a decision that the analysed set of data is not a fractal object.

Analysing a shape of the multi-fractal spectrum, it can be concluded on homogeneity of analysed surfaces. Homogenous surfaces, whose particular fragments do not differ among themselves, are characterized by a narrow spectrum (small difference $\alpha_{max} - \alpha_{min}$), which can be broaden, if a shape of the analysed surface will be more irregular and differentiated in various areas. For the sake of the applied methodology determining the multi-fractal spectrum in the analyzed coatings, it is assumed that its maximum appears for $\alpha = 2$. As values $\alpha < 2$ correspond to probabilities of low values and simultaneously to irregularities of low amplitude so, broadening the multi-fractal spectrum from the left side is characteristic for inhomogeneous surfaces containing tiny grains. Analogically, broadening the spectrum from the right side (for values $\alpha > 2$) it proves that big grains and/or flat areas occur. A positive difference for the spectrum arms height $\Delta f = f(\alpha_{max}) - f(\alpha_{min}) > 0$ proves that in the analysed surface, tiny grains dominate, otherwise ($\Delta f < 0$) high irregularities prevail, defined by high value of probability. Although the multi-fractal spectrum bandwidth is not commonly bound with homogeneity of analysed surface, interpretation of its shape is not unequivocal. The other factors (e.g. roughness, fractal

dimension) influence additionally on values describing appearance of the multi-fractal spectrum. Therefore, values analysing that define a shape of the multi-fractal spectrum received for coatings' surface differed by simultaneously chemical and phase composition, conditions and a type of their obtaining process and substrate's material, on which they were produced is not justified. Problems related to interpretations about shape of the multi-fractal spectrum demand further intensive investigations, nevertheless, still today one can indicate some practical applications, e.g. for quality control and repeatability of coatings' deposition process. Each $\Delta\alpha$ value increase, above or below a certain defined critical value for a given process will be a signal informing about instability of deposition conditions. In case of surface received in conditions differing with one factor change, the multi-fractal analysis can be used to assess its influence on topography of obtained coatings. Quantities for the fractal and multi-fractal analysis and for the quantity value R_{2D} of the analysed coatings are presented in Table 4. On the basis of carried out analyses it can be found that all considered coatings, independently on type of their manufacturing process and the applied substrate's material, show fractal character of surface, what is proved by linear, in defined ranges, the bilogarithmic graphs used for determining the fractal dimension D_s (Fig. 10).

Analysing the acquired results for coatings obtained in the high-temperature CVD process, it was found that their fractal dimension values are situated within 2.015-2.071, whereas roughness R_{2D} within 0.079-0.531 μm. In case of analyzed coatings received in the high-temperature CVD process, there is no dependence between roughness value R_{2D} and the fractal dimension D_s, what results from the fact that high R_{2D} value is connected with surface waviness (irregularity occurrence of high amplitude), and not with proper roughness. Surface inhomogeneity is confirmed by the obtained multi-fractal spectrum bandwidth values ($\Delta\alpha$ = 0.29-0.56), whereas unevenness occurrence of high amplitude – high α_{max} values. For all analyzed coatings obtained in the high-temperature CVD process, a positive difference is received for the height of the multi-fractal spectra arms $\Delta f > 0$.

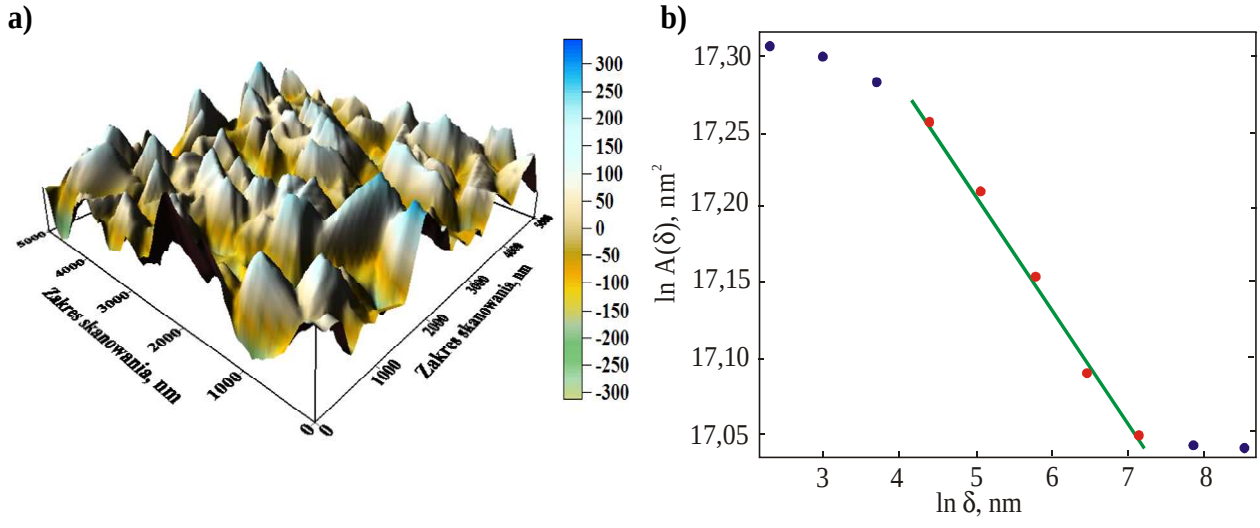

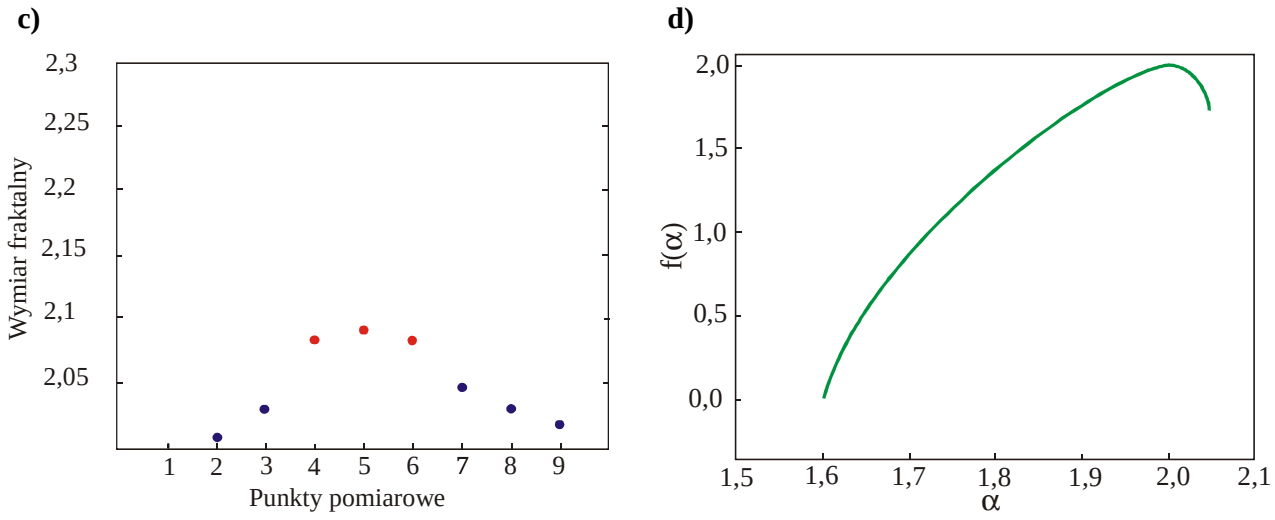

Fig. 10. a) Image of the Ti(C,N)+Al_2O_3 coating surface obtained in the high-temperature CVD process on the Si_3N_4 (AFM, 5 μm) tool ceramics substrate b) bilogarithmic dependence of the approximated area size of the analysed surface on the mesh size used for its determination c) auxiliary diagram indicating the correct points selection on the bilogarithmic plot, and d) multi-fractal spectrum of the analysed coating surface

Table 4. The fractal and multi-fractal analysis results and R_{2D} values for coatings obtained in the high-temperature CVD process and substrate made of tool nitride ceramics Si_3N_4

Substrate's material	Type of coating	R_{2D} [μm]	D_s	α_{min}	α_{max}	$\Delta\alpha$
Si_3N_4	TiN+Al_2O_3	0.098±0.008	2.046±0.005	1.679±0.032	2.067±0.008	0.388±0.033
Si_3N_4	TiN+Al_2O_3+TiN	0.170±0.021	2.034±0.005	1.697±0.054	2.021±0.002	0.325±0.054
Si_3N_4	TiN+Al_2O_3+TiN+Al_2O_3+TiN	0.163±0.019	2.046±0.007	1.657±0.067	2.032±0.003	0.375±0.067
Si_3N_4	Al_2O_3+TiN	0.166±0.022	2.030±0.004	1.550±0.048	2.032±0.006	0.481±0.048
Si_3N_4	TiC+TiN	0.079±0.011	2.014±0.002	1.723±0.051	2.014±0.004	0.291±0.051
Si_3N_4	Ti(C,N)+TiN	0.095±0.012	2.021±0.003	1.681±0.049	2.019±0.015	0.338±0.051
Si_3N_4	Ti(C,N)+Al_2O_3+TiN	0.146±0.017	2.019±0.002	1.708±0.053	2.089±0.008	0.381±0.054
Si_3N_4	Ti(C,N)+Al_2O_3	0.089±0.008	2.071±0.007	1.604±0.041	2.046±0.009	0.442±0.042
Al_2O_3+ZrO_2	TiN+Al_2O_3	0.482±0.039	2.041±0.004	1.570±0.045	2.084±0.011	0.514±0.046
Al_2O_3+ TiC	TiN+Al_2O_3	0.531±0.043	2.039±0.005	1.524±0.052	2.087±0.014	0.563±0.054
Al_2O_3+$SiC_{(w)}$	TiN+Al_2O_3	0.511±0.048	2.028±0.003	1.708±0.031	2.089±0.001	0.381±0.031
Si_3N_4	-	0.031±0.003	2.008±0.001	1.832±0.022	2.005±0.002	0.172±0.022
Al_2O_3+ZrO_2	-	0.060±0.006	2.009±0.001	1.818±0.019	2.007±0.001	0.190±0.019
Al_2O_3+ TiC	-	0.033±0.003	2.009±0.001	1.831±0.023	2.006±0.001	0.175±0.023
Al_2O_3+ $SiC_{(w)}$	-	0.043±0.004	2.008±0.001	1.828±0.021	2.006±0.001	0.178±0.021

A complex method to affect phase composition, being a consequence of chemical composition, the adhesion of analyzed coatings to applied substrate's material correlating with a value of internal stresses, the applied combination of layers, and also a shape of surface decide about obtained mechanical and operational properties. On Fig. 11a and 12a the obtained results are presented for the fractal dimension values and operational properties depending on substrates' materials, including a value of the quantity $\Delta\alpha$. In the event of

coatings obtained in the CVD process it was observed a positive correlation between the fractal dimension value and tool life increase. In case of coatings received in the high-temperature CVD process, for options when outer coating is made of Al_2O_3 high (correlation coefficient r=0.9747) and essential correlation (t=7.557 towards $t_{critical}$=3.182) between the fractal dimension values and tool life increase was found (Fig. 11), similar like for coatings obtained on a substrate made of Si_3N_4 (Fig. 12, correlation coefficient r=0.9575; t=8.136 towards $t_{critical}$=2.447).

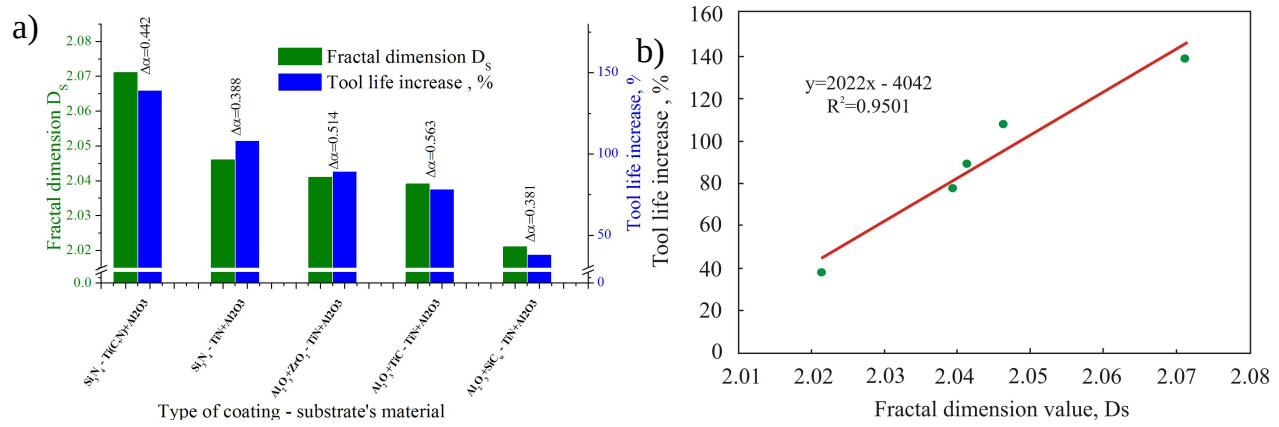

Fig. 11. a) Comparison of obtained results for the fractal dimension values D_s, $\Delta\alpha$ and operational properties b) correlation between tool life increasion and the fractal dimension value for coatings received in the in the high-temperature CVD process (external layer made of Al_2O_3)

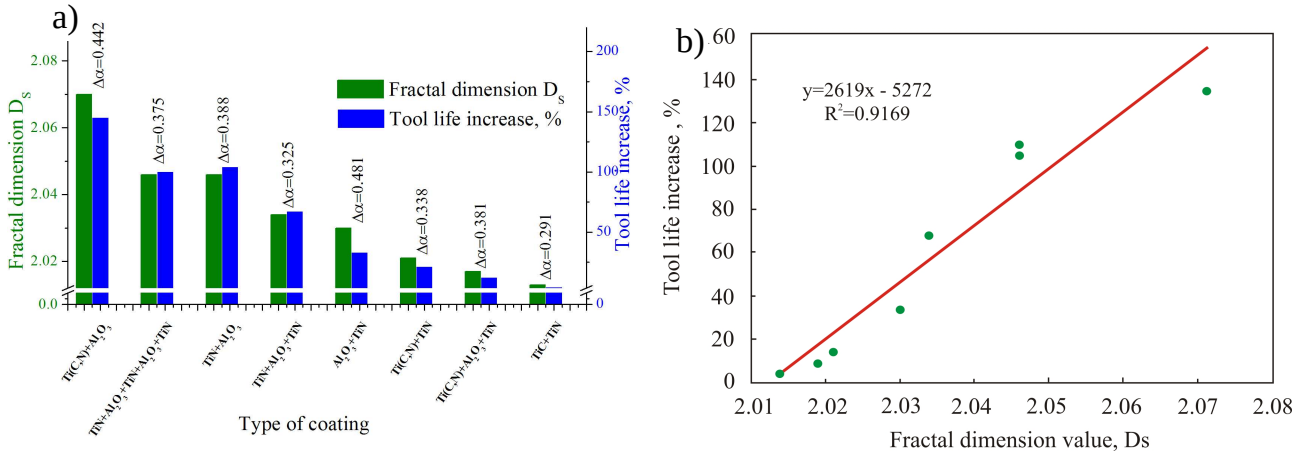

Fig. 12. a) Comparison of obtained results for the fractal dimension values D_s, $\Delta\alpha$ and operational properties b) correlation between tool life increasion and the fractal dimension value for coatings received in the in the high-temperature CVD process (substrate made of nitride ceramics Si_3N_4)

5. CONCLUSIONS

Works [33-35], presenting structural zones models of coatings point out a fact that structure and topography of coating surface decide their mechanical properties, and

consequently, their wear resistance. Employment of the contemporary examination techniques, especially of the scanning electron microscopy and the atomic force microscopy, makes observation of coating surface possible, obtained on tool materials with atomic resolution, however, the results are still used only in a limited range. Fractal geometry is a valuable supplement to analysis methods for results obtained using the atomic force microscopy, rendering it possible to obtain quantitative information characterizing topography of the investigated relationships are mentioned in literature between fractal quantities and roughness [36-38], as well as about fabrication conditions [39-40] of many engineering materials, which was a premise to undertake the research whose goal was employment of the quantitative analysis of surface topography of coatings obtained in the CVD process on tool materials to predict their properties. Based on the obtained experimental studies results the of analyses performed, the following conclusions were formulated:

- For coatings obtained in the high-temperature CVD process prediction of their operational properties based on values of the surface fractal dimension D_s is possible when the external value was made of Al_2O_3 as well as for coatings produced on a substrate made from the Si_3N_4 nitride ceramics.
- Growth of the compression stresses values results in the increased coatings' adhesion substrate material.

REFERENCES

[1] KWAŚNY W., GOŁOMBEK K., DOBRZAŃSKI L.A., 2006, *Multifractal character of surface topography of the coatings on cemented carbides,* Proceedings of the 15th IFHTSE Congress, Vienna-Austria, 532-537.

[2] KWAŚNY W., WOŹNIAK M., MIKUŁA J., DOBRZAŃSKI L.A., 2007, *Structure, physical properties and multifractal characteristics of the PVD and CVD coatings deposition onto the Al_2O_3+TiC ceramics*, Journal of Computional Materials Sciences and Surface Enginering, 1, 97-113.

[3] KWAŚNY W., DOBRZAŃSKI L.A., 2005, *Structure, physical properties and fractal character of surface topography of the Ti+TiC coatings on sintered high speed steel,* Journal of Materials Processing Technology, 164-165, 1519-1523.

[4] KWAŚNY W., DOBRZAŃSKI L.A., PAWLYTA M., GULBIŃSKI W., 2004, *Fractal nature of surface topography and physical properties of the coatings obtained using magnetron sputtering,* Journal of Materials Processing Technology 157-158, 183-187.

[5] MANDELBROT B.B., 1989, *Multifractal measures, especially for the geophysicist,* Pure and Applied Geophysics, 131, 5-42.

[6] RUSS J. C., 1998, *Fractal dimension measurement of engineering surfaces,* International Journal of Machine Tools and Manufacture, 38, 567-571.

[7] XIE H., WANG J.A., STEIN E., 1998, *Direct fractal measurement and multifractal properties of fracture surfaces,* Physics Letters A, 242, 41-50.

[8] BACZMANSKI A., BRAHAM C., SEILER W., SHIRAKI N., (2004) *Multi-reflection method and grazing incidence geometry used for stress measurement by X-ray diffraction,* Surface and Coatings Technology, 182, 43-54.

[9] DUDOGNON J., VAYER M., PINEAU A., ERRE R., 2008, *Grazing incidence X-ray diffraction spectra analysis of expanded austenite for implanted stainless steel,* Surface & Coatings Technology, 202, 5048–5054.

[10] KWAŚNY W., 2009, *A modification of the method for determination of the surface fractal dimension and multifractal analysis,* Journal of Achievements in Materials and Manufacturing Engineering, 33, 115-125.

[11] BOBROWSKI D., 1986, *Probabilistyka w zastosowaniach technicznych,* Wydawnictwo Naukowo-Techniczne, Warszawa.

[12] KAZMANLI M.K., URGEN M., CAKIR A.F., 2003, *Effect of nitrogen pressure, bias voltage and substrate temperature on the phase structure of Mo–N coatings produced by cathodic arc PVD*, Surface and Coatings Technology, 167, 77-82.
[13] CHOWDHURY S., LAUGIER M.T., HENRY J., 2007, *XRD stress analysis of CVD diamond coatings on SiC substrates*, International Journal of Refractory Metals & Hard Materials, 25, 39-45.
[14] ŁĄGIEWKA E., 2007, *Projektowanie i wytwarzanie funkcjonalnych materiałów gradientowych-opracowanie metod charakteryzowania struktury i właściwości materiałów gradientowych*, PAN, Kraków, 151-176.
[15] AHLGREN M., BLOMQVIST H., 2005, *Influence of bias variation on residua stress and texture In TiAlN PVD coatings*, Surface Coatings Technology, 200, 157-160.
[16] WELZEL U., LIGOT J., LAMPARTEM P., VERMEULEN A.C., MITTEMEIJER J., 2005, *Stress analysis of polycrystalline thin films and surface regions by X-ray diffraction*, Journal pf Applied Crystalography, 38, 1-29.
[17] LENCZYK D., 2005,Podstawy tensometrii rentgenowskiej, Wydawnictwo Politechniki Poznańskiej.
[18] VAN HACKER K., DE BUYSER L., CELIS J.P., VAN HOUTTE P., 1994, *Charackterization of thin nickiel electrocoatings by the low-incident-beam-angle diffraction method*, Journal of Applied Crystallography, 27, 56-66.
[19] QUAEYHAEGENS C., KNUYT G., STALS L.M., 1995, *Study of the residual macroscopic stress in TiN coatings deposited on various steel type*, Surface and Coatings Technology, 74-75, 104-109.
[20] SKRZYPEK S. J., 2002, *Nowe możliwości pomiaru makronaprężeń własnych materiałów przy zastosowaniu dyfrakcji promieniowania X w geometrii stałego kąta padania*, Uczelniane Wydawnictwo Naukowo-Dydaktyczne, Kraków.
[21] WROŃSKI S., WIERZBANOWSKI K., BACZMAŃSKI A., BRAHAM C. H., LODINI A., 2008, *Corrections for residua stress in X-Ray grazing incidence technique*, Archives of Metallurgy and Materials, 53, 225-281.
[22] MA C-H., HUANG J-H., CHEN H., 2002, *Residual stress measurement in textured thin film by grazing-incidence X-ray diffraction*, Thin Solid Films, 418, 73-78.
[23] THORNTON J. A., HOFFMAN D.W., 1986, *Stress-related effects in thin films*, Thin Solid Films, 171, 5-31.
[24] CICHOSZ P., 2006, Narzędzia skrawające, Wydawnictwo Naukowo-Techniczne, Warszawa.
[25] HOGMARK S., JACOBSON S., LARSSON M., 2000, *Design and evaluation of tribological coatings*, Wear, 246, 20-33.
[26] FALLQVIST M., OLSSON M., RUPII S., 2007, *Abrasive wear of multilayer Al_2O_3–Ti(C,N) CVD coatings on cemented carbide*, Wear, 263, 74-80.
[27] XIE H., WANG J-A., KWASNIEWSKI M.A., *Multifractal characterization of rock fracture surfaces*, International Journal of Rock Mechanics and Mining Sciences (1999) 19-27.
[28] ZHOU H.W., XIE H., 2004, *Anisotropic characterization of rock fracture surfaces subjected to profile analysis*, Physics Letters A, 355-362.
[29] LIANG B., SHI Y., HARTEL R.W., 2008, *Correlation of Rheological and Microstructural Properties in a Model Lipid System*, Journal of the American Oil Chemists' Society, 85, 397–404.
[30] ZHOU Z., LIU S., CHU L., GU L., 2003, *Fractal analysis of worn surfaces of ZnO whisker/natural rubber-styrene butadiene rubber-butyl rubber composites*, Journal of Applied Polymer, 90, 667 – 670.
[31] XIE H., GAO F., 2000, *The mechanics of cracks and a statistical strength theory for rocks*, International Journal of Rock Mechanics and Mining Sciences, 37, 477-488.
[32] STACH S., ROSKOSZ S., CYBO J., CWAJNA J., 2003, *Multifractal description of fracture morphology: investigation of the fractures of sintered carbides*, Materials Characterization, 51, 87-93.
[33] THORNTON J.A., 1986, *The microstructure of sputter-deposited coatings*, Journal of Vacuum Science Technology A 4, 3059-3065.
[34] MESSIER A. P., GIRI A.P., ROY R.A., 1984, *Revised structure zone model for thin film physical structure*, Journal of Vacuum Science and Technology, 2, 500-5003.
[35] MOVCHAN B.A., DEMCHISHIN A.V., 1969, *Fizika Metallov i Metallovedenie*, 28, 653-656.
[36] SUN X., FU Z., WU Z., 2002, Fractal processing of AFM images of rough ZnO films. Materials Characterization, 48, 169–175.
[37] REISEL G., HEIMANN R.B., 2004, *Correlation between surface roughness of plasma-sprayed chromium oxide coatings and powder grain size distribution: a fractal approach*. Surface & Coatings Technology, 185, 215–221.
[38] RISOVIC D., MAHOVIC S., GOJO M., 2009, *On correlation between fractal dimension and profilometric parameters in characterization of surface topographies*, Applied Surface Science, 255, 4283–4288.
[39] CHEN Z.W., LAI J.K.L., SHEK C.H., 2005, *Multifractal spectra of scanning electron microscope images of SnO_2 thin films prepared by pulsed laser deposition*, Physics Letters A, 345 218-223.
[40] LAM K.T., JI L.W., 2007, *Fractal analysis of InGaN self-assemble quantum dots grown by MOCVD*. Microelectronics Journal, 38/8-9, 905-909.